# A Battery-Less Thermoelectric Energy Harvesting Interface Circuit With 35 mV Startup Voltage

Yogesh K. Ramadass and Anantha P. Chandrakasan, *Fellow, IEEE*

***Abstract*—A battery-less thermoelectric energy harvesting interface circuit to extract electrical energy from human body heat is implemented in a 0.35 $\mu$m CMOS process. A mechanically assisted startup circuit enables operation of the system from input voltages as low as 35 mV. An efficient control circuit that performs maximal transfer of the extracted energy to a storage capacitor and regulates the output voltage at 1.8 V is presented.**

***Index Terms*—Energy harvesting, low voltage startup, maximum power point tracking, micro-power DC-DC converters, thermoelectric energy harvesters.**

## I. Introduction

SOPHISTICATED battery operated electronic systems and self-powered devices have found diverse applications recently existing as autonomous or hand held objects in every environment around us and in some cases even within us. The stellar advances in CMOS process technologies and circuit techniques have reduced the power consumption of circuits far enough to enable a new class of self-powered systems. Emerging applications like wireless micro-sensor networks, implantable and wearable medical electronics and industrial automation sensors are severely energy constrained. It is often impractical to operate these systems on a fixed energy source like a battery owing to the difficulty in replacing the battery. A 1 $cm^3$ primary lithium battery has a typical energy storage capacity of 2800 J [1]. This can potentially supply an average electrical load of 100 $\mu$W for close to a year but is insufficient for systems where battery replacement is not an easy option. The ability to harvest ambient energy through energy scavenging technologies is necessary for battery-less operation. The most common harvesters transducer solar, vibrational or thermal energy into electrical energy. In all of these systems, long operational lifetimes and low cost are highly important. Energy efficiency of the integrated circuits within these systems plays a major factor in determining the size, weight, cost and lifetime. Accordingly, highly aggressive low-power circuit design and efficient power delivery is required to meet the power constraints set by the system.

Manuscript received April 20, 2010; revised July 19, 2010; accepted July 30, 2010. Date of publication October 14, 2010; date of current version December 27, 2010. This work was supported in part by the MIT Energy Initiative. This paper was recommended by Guest Editor Alison Burdett.

The authors are with the Massachusetts Institute of Technology, Cambridge, MA 02142 USA (e-mail: ryogesh@alum.mit.edu).

Color versions of one or more of the figures in this paper are available online at http://ieeexplore.ieee.org.

Digital Object Identifier 10.1109/JSSC.2010.2074090

To minimize power consumption of the electronic devices, significant research has targeted the load circuits like radios and DSP's, where process scaling coupled with circuit techniques like voltage scaling, parallelism etc. have reduced power consumption of circuits dramatically down to less than 10 mW. But this reduction in power does not map onto an equivalent improvement in operating lifetime. This is because the end circuits are interfaced to the energy source through intermediate energy management circuits. Unless these intermediate circuits can maintain good efficiency over these low power ranges, proportional savings cannot be attained. This becomes a key bottleneck in low power systems. Also, in the case of energy harvested applications where the battery can be eliminated altogether, a new breed of challenges are introduced that conventional power management techniques more suited for battery operated systems do not handle well. Specifically, for these systems while the efficiency of the internal blocks are important, the ultimate metric is the overall energy extractable from the transducers.

Harvesting ambient heat energy using thermoelectric generators (TEGs) [2]–[4] is a convenient means to supply power to body-worn and industrial sensors. Using TEGs for body-wearable applications limits the output voltage to 50 mV for temperature differences of 1–2 K usually found between the body and ambience. Several existing systems [5], [6] use a battery or an initial high voltage energy input to kick-start operation of the system from this low voltage. Further, changing external conditions cause the voltage and power generated by the TEG to vary, necessitating efficient control circuits that can adapt and extract the maximum possible power out of these systems. In this paper, a battery-less thermoelectric energy harvesting interface circuit which uses a mechanically assisted startup circuit to operate from 35 mV input is presented. An efficient control circuit that performs maximal end-to-end transfer of the extracted energy to a storage capacitor and regulates the output voltage at 1.8 V is demonstrated.

## II. Thermoelectric Energy Harvesters

A thermoelectric element converts thermal energy in the form of temperature differences into electrical energy and vice-versa. The fundamental physical process involved in thermoelectrics is the Seebeck effect. The basic construction unit of a thermal harvester is a thermocouple. The thermocouple is composed of an n-type material electrically in series with a p-type material. When a temperature difference is applied across this material, heat begins to flow from the hotter to the cooler side. In the process, the energy from the applied heat allows the free electrons and holes to move and form an electric potential and cause current to flow if the circuit is closed. Commonly used thermal

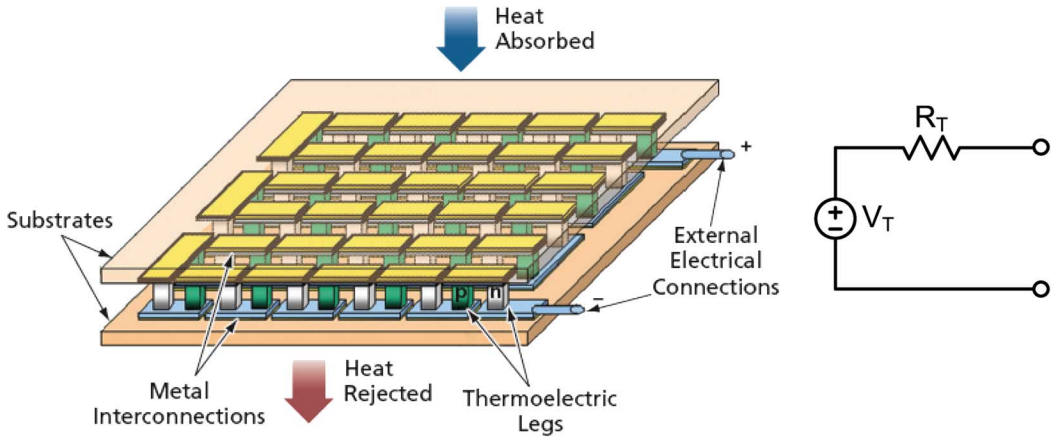


Fig. 1. A typical thermoelectric generator and its electrical equivalent circuit.

harvesters for power generation consist of p- and n-doped Bismuth telluride owing to its superior thermal properties. One p-n leg of this material generates around 0.2 mV/K difference between the hot and cold sides. To boost the voltage output by the harvester, a typical thermoelectric device includes multiple n-type and p-type thermoelectric legs sandwiched between two high-thermal-conductivity substrates as shown in Fig. 1. The n- and p-type legs are electrically connected in series by alternating top and bottom metal contact pads to form a thermopile. The Seebeck effect in the n-type material creates a flow of excess electrons from the hot junction to the cold junction. In the p-type material, holes migrate toward the cold side creating a net current flow which is in the same direction as that of the n-type material.

The voltage obtained at the output of the thermal harvester is proportional to the temperature difference across the thermoelectric element. Electrically, the thermal harvester can be modeled as a voltage source in series with a resistance as shown in Fig. 1. The open-circuit voltage can be expressed as $V_T = S.\Delta T$ where S is the Seebeck coefficient of the thermopile and $\Delta$T is the temperature difference applied across the harvester. The resistance arises from the metal interconnections and the resistance along the pellets. For a 10 cm$^2$ device, this series combination of p- and n-legs provides around 25 mV/K of temperature difference [7] applied across the harvester. This poses a major problem while using thermoelectric harvesters for body worn applications powered by human heat because of the small temperature differences (2–3 K) available. The thermal harvester outputs only 50–75 mV of open-circuit voltage. It is not possible to use this voltage to directly power CMOS circuits in the absence of a battery. The next section presents a mechanically assisted startup circuit that helps to interface CMOS circuits directly with the thermal generator without the aid of a battery.

## III. Low Voltage Startup

Since thermoelectric harvesters for body-wearable applications output an extremely low voltage, startup circuits are essential to generate higher voltages for proper functioning of the interface circuitry. [8] presents a circuit that is completely electronic and can startup from voltages as low as 20 mV without the help of a battery. While this circuit does not need other peripherals to assist startup, it needs a bulky transformer with a large turns ratio and an external N-channel JFET to achieve startup from low voltages, and hence is not very well suited to portable applications. [9] proposed using Reed switches and tunnel diodes to assist in the startup operation. The authors were able to demonstrate startup from 200 mV. Starting up from even lower voltages is a problem with tunnel diodes, while Reed switches suffer from reliability issues. A discrete low-voltage boost converter circuit that starts up from 0.7 V using an external mechanical switch was presented in [10]. The boost converter circuits presented in [5], [11] use traditional inductor-based or charge pump boost circuits that require atleast 0.6 V to startup.

The problem with thermoelectric inputs is that the voltage it outputs for temperature differences normally observed is around 50–75 mV. It is not possible to operate CMOS switches directly out of these low voltages to use conventional boosting techniques. The voltage available needs to be close to 1 V to suitably operate CMOS switches in the technology used in this implementation to achieve efficient voltage boosting. Since the interface circuit designed is intended for body-wearable applications, the movement of humans presents small amount of ambient mechanical vibrations. These vibrations are put into use in a mechanically assisted startup circuit shown in Fig. 2. The switch $S1$ shown in the figure is a mechanical switch which turns ON and OFF on the application of very small amount of vibration of less than 0.1 g in acceleration. The vibrations can be induced when the device is worn on the arm or on the body of a person. When the switch $S1$ is ON, the voltage available from the thermoelectric harvester causes current to flow in the inductor $L$. When the switch turns OFF, the current in the inductor has to find an alternate path to flow. This causes the transistor $M1$ which is connected as a diode to turn ON, and the energy flows into the capacitor $C_{\rm DD}$. If the diode is considered ideal, assuming that there was no initial voltage across $C_{\rm DD}$, the voltage obtained at $C_{\rm DD}$ at the end of the ON/OFF cycle is

$$V_C(final) = \frac{\sqrt{L/C_{\rm DD}}}{R_T + R_L + R_{SW}} V_T = Q_T V_T \qquad (1)$$

where $Q_T$ is the $Q$-factor of the startup network, $R_T$ is the internal resistance of the thermoelectric harvester, $R_L$ and $R_{SW}$

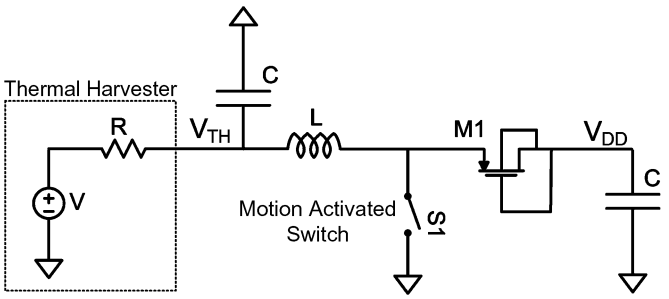


Fig. 2. A mechanically assisted startup circuit to kick start electrical energy extraction from the TEG.

are the parasitic series resistances of the inductor and the switch. This can be derived by equating the energy stored in the inductor when the switch $S1$ is ON to the energy in the capacitor when the inductor current reaches zero. With a 30 mV input, $Q_T$ needs to be at least 34 to get more than 1 V across $C_{\rm DD}$. However, the diode formed by $M1$ is not ideal and has a voltage drop across it. Hence, $Q_T$ needs to be higher than 34 to get 1 V across $C_{\rm DD}$. In the presence of diode losses, the voltage across the capacitor comes up to

$$V_C(final) = \sqrt{V_D^2 + Q_T^2 V_T^2} - V_D. \tag{2}$$

If we assume a $V_D$ of 0.6 V, then with a $Q_T$ of 42, the input open circuit voltage needs to be at least 35 mV to obtain a 1 V output. The value of $L$ used is 22 $\mu$m and that of $C_{\rm DD}$ is 470 pF. The thermal harvester has a resistance of 5 $\Omega$, and the parasitic resistances add up to 150 m$\Omega$. This gives a $Q_T$ of 42. The voltage gain can be increased by increasing $L$ or decreasing $C_{\rm DD}$. Increasing $L$ too much increases the size of the system and cost. $C_{\rm DD}$ on the other hand cannot be decreased arbitrarily as it needs to have a moderate amount of energy to power circuits. Reducing $V_D$ also helps in decreasing the input voltage required for startup. This is however process dependent. Synchronous rectifiers are not possible during startup due to the lack of suitable voltage to turn ON the switches. 35 mV of open-circuit voltage corresponds to a temperature difference of 1.5 K across the thermoelectric harvester, which can be achieved in body-worn applications.

## IV. Startup Block and Associated Control

Once $V_{\rm DD}$ reaches 1 V, the electronics within the startup block are activated and the mechanical switch is needed no more. The circuits within the startup block are shown in Fig. 3. The internal clock and reference generator blocks are activated first and are both powered by $V_{\rm DD}$. The reference voltage generator block generates the voltage $V_{REF}$ which is used as the reference voltage throughout the circuit. The voltage $V_{REF}$ is pegged close to 0.7 V once $V_{\rm DD}$ goes above 1 V. $V_{\rm DD}$ simultaneously powers an internal clock generator block. The clock generator consists of multiple delays arranged to form a ring oscillator. The $CLK$ signal feeds the comparator block which compares a divided version of $V_{\rm DD}$ with $V_{REF}$. For the moment, assume that the signal $VDD\_VL\_SHORTb$ is at '0'. The purpose of this signal is explained in Section VII-A. The resistance ratio is set such that if $V_{\rm DD}$ is less than 1.8 V, the clocked comparator triggers the $CHG\_VDD$ signal which is used to transfer energy from the thermal input on to $C_{\rm DD}$. When $CHG\_VDD$ goes high, the CMOS switch $M2$ turns ON and causes current to flow in the inductor $L$. $CHG\_VDD$ going low turns the switch $M2$ OFF thereby turning on the diode $M1$ and charging $C_{\rm DD}$. This process repeats whenever $V_{\rm DD}$ falls below 1.8 V. Fig. 4 shows simulated voltage waveforms of the startup block in operation. The moment the mechanical switch $S1$ turns OFF, $V_{\rm DD}$ rises to above 1 V. This starts up the reference voltage block where $V_{REF}$ rises close to 0.7 V. The clock generator block together with the comparator is also enabled and this makes the $CHG\_VDD$ signal go high whenever $V_{\rm DD}$ is less than 1.8 V at the rising edge of the $CLK$ signal. The $V_{\rm DD}$ signal is regulated to 1.8 V by using ON-OFF control of the comparator. The ripple on the $V_{\rm DD}$ supply is high due to the low value of $C_{\rm DD}$. The mechanical switch is needed only once in the system for startup.

## V. Thermoelectric Energy Harvesting System Architecture

The overall architecture of the thermoelectric energy harvesting system is shown in Fig. 5. The startup circuit starts the system operation from a completely OFF state where the voltage in all the main capacitors is below usable values. At this point, a mechanical vibration due to human motion triggers switch $S1$ which enables the startup block to charge $C_{\rm DD}$ above 1 V as explained in the previous section. This triggers an internal clock generator within the start block which powers CMOS switches to help pump in further charge into $C_{\rm DD}$ through the inductor $L$. This process repeats as long as $V_{\rm DD}$ is less than 1.8 V. Once $V_{\rm DD}$ reaches 1.8 V, the storage block is activated. This turns on the storage part of the system. The storage capacitor $C_{STO}$ is designed to be much larger than $C_{\rm DD}$. The storage block shown in Fig. 5 is necessary to act as a buffer to energy obtained from the thermoelectric harvester. We cannot use the voltage $V_{\rm DD}$ to directly power load circuits because by design, the value of $C_{\rm DD}$ is very small. The voltage across $C_{\rm DD}$ would drain very fast on connecting a significant load current across it. When $V_{\rm DD}$ goes above 1.8 V, the power from the thermoelectric harvester is diverted towards $C_{STO}$. This builds up the voltage $V_{STO}$. The voltage $V_{STO}$ varies depending on the power available from the thermoelectric harvester and the power consumed by the load. Hence, it cannot be used to directly power load circuits. To give a constant voltage to load circuits, a DC-DC buck converter is used after the storage capacitor to transfer energy to the load at a constant voltage. The DC-DC converter block is only activated after $V_{STO}$ goes above 2.4 V. $V_{\rm DD}$ is used as the control voltage for both the storage and DC-DC converter blocks. The DC-DC converter is used to regulate $V_L$ to 1.8 V. Once, $V_L$ reaches 1.8 V, the capacitors $C_{\rm DD}$ and $C_L$ are shorted together to improve the energy harvesting efficiency of the thermoelectric harvester. The reason for this is explained in Section VII-A.

## VI. Storage Block

Any power delivery system where the rate of flow of energy into and out of the system are different and variable over long

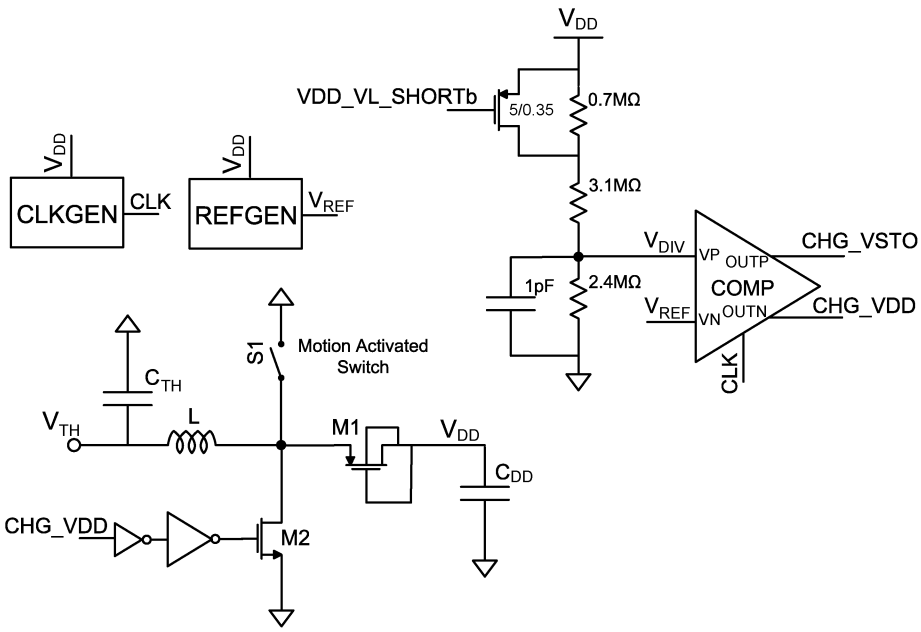


Fig. 3. Circuit elements within the startup block. $VDD\_VL\_SHORTb$ is at $V_{\rm DD}$ during the startup process.

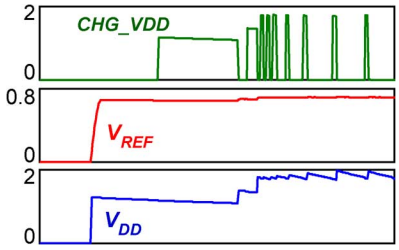


Fig. 4. Simulated waveforms showing the functioning of the startup block.

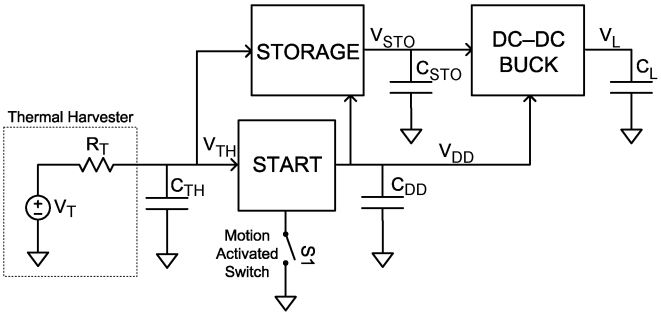


Fig. 5. Architecture of the thermoelectric energy harvesting system.

periods of time needs an intermediate storage unit to act as a buffer to efficiently use the energy available. In the case of the thermoelectric harvester, it is prudent to extract the energy available from the thermal harvester irrespective of whether the load circuit needs it at that point of time or not. This excess energy can be stored and used at a later time when the load demands increase. A storage block that acts as a buffer needs a large amount of capacitance to smoothen the instantaneous power spurts. The storage block shown in Fig. 6 is used as the buffer in the thermoelectric energy harvesting interface circuit. The power flow path from the thermal harvester to the storage capacitor $C_{STO}$ is similar to that in the startup block. A mechanical switch is not necessary in the storage block because by the time the storage block is activated, there is enough energy across $C_{\rm DD}$ to power the electronics. The storage block is activated when $V_{\rm DD}$ goes above 1.8 V. During the rising edge of a $CLK$ signal, if the comparator in Fig. 3 senses that $V_{\rm DD}$ is greater than 1.8 V, the $CHG\_VSTO$ signal goes high which turns on transistor $M4$ of the storage block. This causes current to flow in the inductor $L_{STO}$. Once $CHG\_VSTO$ goes low, the switch $M4$ turns OFF. Unlike the start block, the switch $M3$ in the storage block is not configured as a diode. The switch is turned ON strongly using the $PG$ signal for better efficiency. This is possible with the storage block because, by the time the storage block is activated, there is enough voltage across $C_{\rm DD}$ to actively turn-ON CMOS switches. The switch $M4$ needs to be ON long enough for the current in $L_{STO}$ to reach zero. It should then turn OFF. The comparator COMP2 together with the PULSEGEN block takes care of the timing and width of the $PG$ pulse to achieve zero-current switching of the inductor current.

### A. Closed-Loop Zero-Current Switching Control

To achieve zero-current switching (ZCS) of the current in inductor $L_{STO}$, the time for which the switch $M4$ is ON ($\tau_{\rm N}$) is related to the time for which the switch $M3$ is ON ($\tau_{\rm P}$) by

$$\frac{\tau_P}{\tau_N} = \frac{V_{TH}}{V_{STO} - V_{TH}}. \tag{3}$$

In this relation, both the voltages $V_{TH}$ and $V_{STO}$ are variable. This prevents us from using the open-loop approximate zero-current switching technique described in [12]. Hence, to achieve ZCS, closed-loop control is employed in this design. The time for which the nMOS transistor $M4$ is ON is fixed by setting it to be equal to the pulsewidth of the $CHG\_VSTO$ signal, which is one-half the time period of the $CLK$ signal. To achieve ZCS, the width of $PG$ ($\tau_{\rm P}$) needs to be equal to that given by (3). This is achieved by observing the voltage

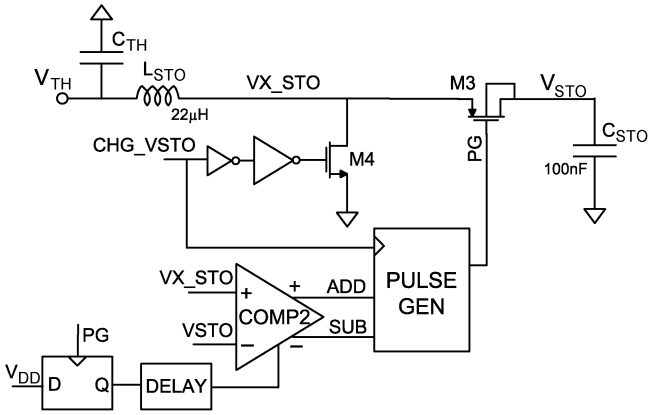


Fig. 6. Storage circuit to transfer energy from the thermal harvester to the storage capacitor $C_{STO}$. The comparator and pulse generator help to achieve closed loop zero-current switching of the current through $L_{STO}$.

at the node $VX\_STO$ immediately after the switch $M3$ is turned OFF. If the switch $M3$ is turned OFF too quick, i.e., if the pulsewidth $\tau_{\rm P}$ is lower than that required, the remaining inductor current in $L_{STO}$ turns ON the parasitic diode across $M3$. This forces the voltage at $VX\_STO$ to go above $V_{STO}$. On the other hand, if the switch $M3$ is turned OFF too late, the inductor current reverses direction. This drains the parasitic capacitor on the drain node first before turning ON the parasitic diode across $M4$. This forces the voltage $VX\_STO$ to go below $V_{STO}$ first and eventually to below zero if $\tau_{\rm P}$ is too large. Thus, by comparing $VX\_STO$ with $V_{STO}$, we can determine whether the pulsewidth $\tau_{\rm P}$ is larger or smaller than necessary. This is precisely what the comparator COMP2 detects. The comparison takes place a fixed delay after the rising edge of $PG$. Depending on whether $VX\_STO$ is higher or lower than $V_{STO}$, either the $ADD$ or $SUB$ pulse goes high. Based on this, the PULSEGEN block suitably increases or decreases the width of $PG$ to achieve zero-current switching of the inductor current. A more detailed explanation of the PULSEGEN block is provided in [13].

### B. Maximum Power Extraction Methodology

The description till now has been about how to startup the thermal energy harvesting circuit and to transfer power from the harvester on to the storage capacitor. No mention has been made about the amount of power being transferred. The maximum power that can be obtained from the thermoelectric harvester shown in Fig. 1 can be given by

$$P_{max} = \frac{V_T^2}{4R_T}. \tag{4}$$

This follows directly from the maximum power transfer theory. To get this maximum power, the load circuit following the thermoelectric harvester needs to present an impedance equal to $R_T$. Equivalently, we can extract maximum power available if the output voltage of the harvester $V_{TH}$ is regulated close to $V_T/2$. This is achieved with the help of a control strategy described here. Consider Fig. 6 where the switch $M4$ is constantly switched ON and OFF with the help of the $CHG\_VSTO$ signal. The $CHG\_VSTO$ signal is generated by a comparator clocked at frequency $f_s$. Thus, if the comparator triggers $CHG\_VSTO$ at every cycle, then the frequency of $CHG\_VSTO$ is also $f_s$. Let the pulsewidth of the ON-time of $CHG\_VSTO$ be $\tau_{\rm N}$. This means that the time for which $M4$ is ON every cycle is $\tau_{\rm N}$. In steady state, $V_{STO}$ is regulated to be much higher than $V_{TH}$. Thus, the time for which the switch $M3$ is ON is very small compared to $\tau_{\rm N}$. This can be seen from (3). This being the case, the energy delivered to $C_{STO}$ every cycle assuming ideal blocks can be approximately given by

$$E_{cycle} = \frac{V_{TH}^2 \tau_N^2}{2L_{STO}}. \tag{5}$$

This repeats every cycle and hence the power delivered to $C_{STO}$ is given by

$$P_{STO} = E_{cycle} f_s = \frac{V_{TH}^2 \tau_N^2}{2L_{STO}} f_s. \tag{6}$$

In steady state, the power delivered to $C_{STO}$ should be equal to the power extracted from the thermoelectric harvester. Hence, to extract the maximum power, on equating (4) and (6), we get the following:

$$\frac{V_{TH}^2}{R_T} = \frac{V_{TH}^2 \tau_N^2}{2L_{STO}} f_s \Rightarrow \tau_N^2 f_S = \frac{2L_{STO}}{R_T}. \tag{7}$$

Since $\tau_{\rm N}$ is designed to be one half the period of the $CLK$ signal, the condition on $f_s$ to achieve maximum power transfer can be given by

$$f_S = \frac{R_T}{8L_{STO}}. \tag{8}$$

Thus, if we can design $f_s$ suitably for a given $L_{STO}$ and $R_T$, we can extract maximum power available from the thermoelectric harvester. For an $R_T$ of 5 $\Omega$ and an $L_{STO}$ of 22 $\mu$m, $f_s$ should be 28.4 kHz. The clock generator block shown in Fig. 3 is designed to output a $CLK$ with the above mentioned frequency in the nominal state. Extra bits of control [13] are provided in the clock generator block not only to account for process variations but also to adjust the clock frequency with change in $R_T$ and $L_{STO}$. A major advantage of this method is that once a suitable thermoelectric harvester and inductor have been picked, the clock frequency can be set to achieve maximum power transfer. This is a simple way to get the maximum power out, instead of using more complex maximum power tracking loops. Also, it has the additional advantage that even when $V_T$ moves around due to temperature variations, since (8) is independent of $V_T$, the circuit will settle itself at the maximum power point.

## VII. Architecture of the DC-DC Converter

The final block of the thermoelectric energy harvesting system is the DC-DC buck converter. The voltage $V_{STO}$ at the output of the storage block cannot be used to power circuits directly because it is unregulated and can vary with change in input and output power. To provide a clean regulated supply to the load circuits, a DC-DC converter is necessary. The architecture of the DC-DC buck converter is shown in Fig. 7. The buck converter employs pulse-frequency modulation mode of control to regulate $V_L$. All the comparators used in the DC-DC converter are clocked and are similar to the one used in the startup

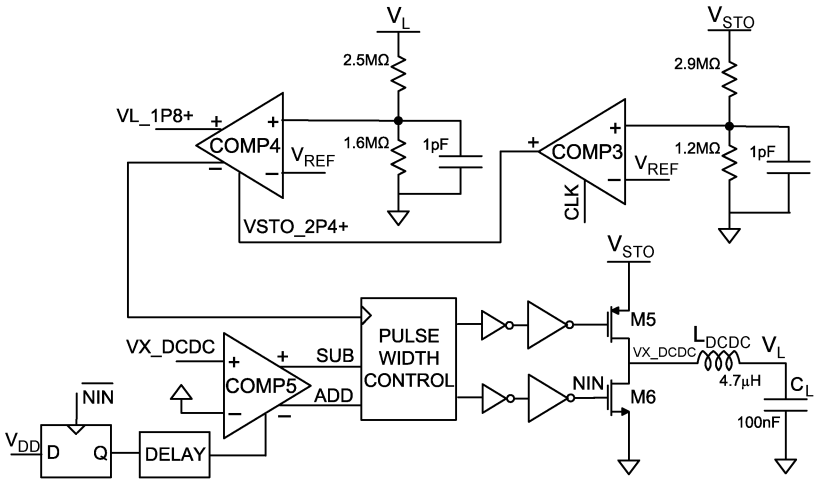


Fig. 7. Architecture of the buck DC-DC converter to provide a regulated 1.8 V output. The buck converter gets activated only after $V_{STO}$ goes above 2.4 V.

block. The comparator COMP3's output feeds the clock to the comparator COMP4. The DC-DC converter is designed to be activated only when $V_{STO}$ is above 2.4 V. The first comparator does this function by comparing a suitably divided version of $V_{STO}$ with the reference voltage $V_{REF}$. Only when $V_{STO}$ goes above 2.4 V does the signal $VSTO\_2P4+$ get activated. This essentially gates the clock to comparator COMP4 when $V_{STO}$ is less than 2.4 V thereby disabling the DC-DC buck converter.

The second comparator COMP4 is used to regulate $V_L$ to 1.8 V. The value of the output voltage is set to 1.8 V in this design, but this can be easily changed by changing the resistances of the ladder network of COMP4. When $V_L$ falls below 1.8 V, the comparator sends a pulse to the pulse-width control block which turns ON the power transistors to transfer charge from $V_{STO}$ to $V_L$. The pulse-width control block employs closed-loop control to achieve ZCS similar to the methodology described in Section VI-A. However, since the control here is for a buck converter rather than a boost converter, the ZCS block is slightly different. Here, the voltage at the drain nodes of the power transistors $VX\_DCDC$ is compared to ground instead of $V_{STO}$. The comparison takes place immediately after the nMOS power transistor is turned OFF. If the nMOS transistor is turned OFF too quick, the remaining inductor current in $L_{DCDC}$ turns ON the parasitic diode across the nMOS transistor. This forces the voltage at $VX\_DCDC$ to fall to a diode drop below ground. On the other hand, if the nMOS transistor is turned OFF too late, the inductor current reverses direction and hence the parasitic diode across the pMOS transistor turns ON after the parasitic capacitance at the drain node gets charged to $V_{STO}$. This forces the voltage $VX\_DCDC$ to go above $V_{STO}$. Thus, by comparing $VX\_DCDC$ with ground, we can determine whether the nMOS pulse-width is larger or smaller than necessary. This is precisely what comparator COMP5 detects. The comparison takes place a fixed delay after the falling edge of $NIN$. Depending on whether $VX\_DCDC$ is higher or lower than ground, either the $SUB$ or $ADD$ pulse goes high. Based on this, the pulsewidth control block suitably increases or decreases the width of $NIN$ to achieve zero-current switching of the inductor current. A more detailed explanation of the pulsewidth control block is provided in [13].

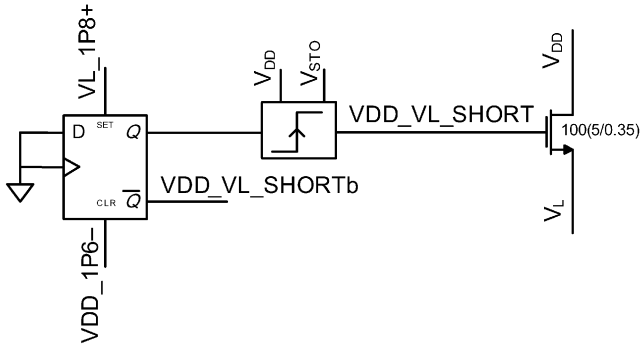


Fig. 8. Circuit used to short $V_{\rm DD}$ and $V_L$.

### A. Disabling the Start Block

Once $V_L$ reaches 1.8 V, the $VL\_1P8+$ signal shown in Fig. 7 goes high. This is used to activate the $VDD\_VL\_SHORT$ signal that is used to short the capacitors $C_L$ and $C_{\rm DD}$ as shown in Fig. 8. Simultaneously the signal $VDD\_VL\_SHORTb$ goes high which changes the threshold of comparison for comparator COMP1 in Fig. 3 to 1.6 V. Since $V_L$ and $V_{\rm DD}$ are just above 1.8 V at this stage, the $CHG\_VDD$ signal in Fig. 3 never gets triggered. This helps to keep the storage circuit active all the time instead of time-sharing it with the start circuit. The power to $V_{\rm DD}$ flows through the storage block and not directly from the thermal harvester. Hence, the time sharing of the thermal input between the start and storage blocks can be avoided. Also, since the storage circuit will now switch at a constant frequency determined by the maximum power transfer considerations described in Section VI-B, optimal operation of the thermoelectric energy harvester circuit is possible. This also helps in the overall efficiency of the system because transferring power to $V_{\rm DD}$ through the startup block is inefficient owing to using a free-wheeling diode. The shorting is disabled once the voltage $V_{\rm DD}$ falls below 1.6 V.

## VIII. Measurement Results

The thermoelectric energy harvester interface circuit was implemented in a 0.35 $\mu$m CMOS process. Fig. 9 shows the die photo of the test chip. The active area of the startup, storage

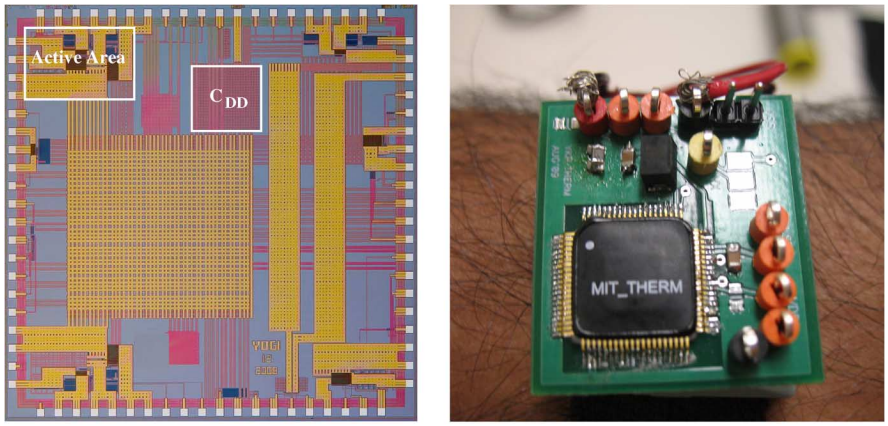


Fig. 9. (a) Die photo of the thermal energy harvesting interface circuit identifying the area consumed by the active blocks and the startup capacitor $C_{DD}$. (b) The thermal harvesting chip worn on the arm of a person. The PCB occupies 7.5 $cm^2$ in area.

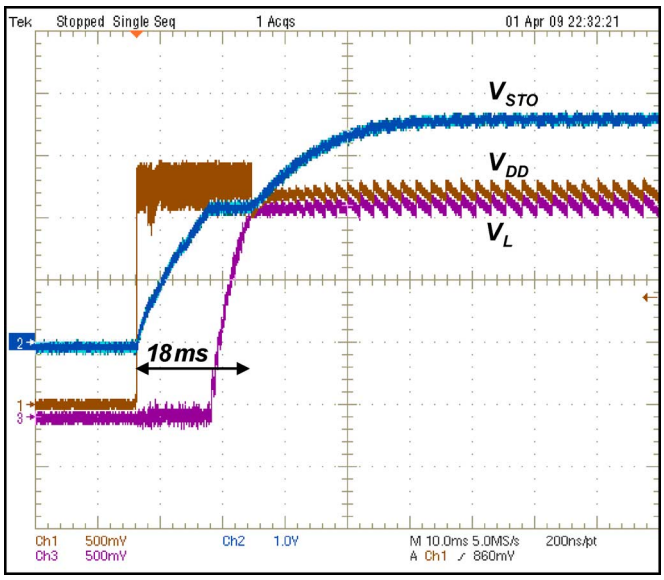


Fig. 10. Measured waveforms of the voltages within the thermal harvesting circuit during startup from a 50 mV input voltage.

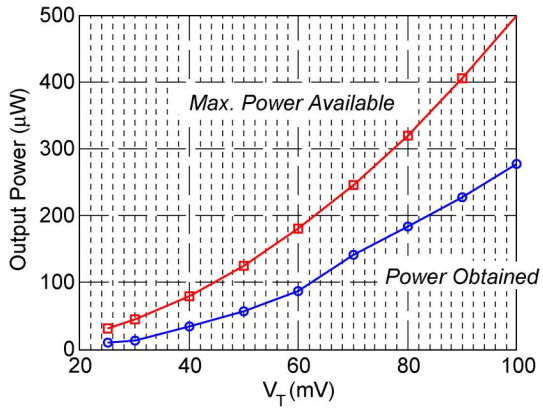


Fig. 11. Measured electrical power obtained at the output of the buck converter compared to the maximum power available from the thermal harvester.

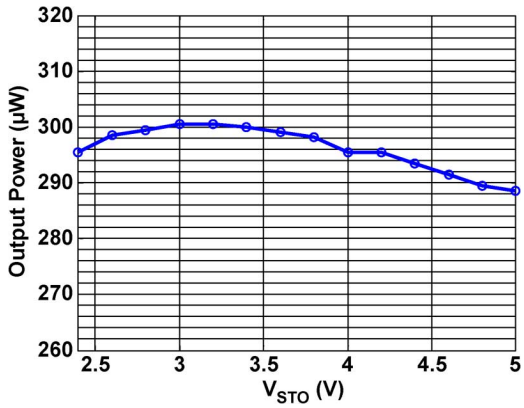


Fig. 12. Measured electrical power obtained at the output of the storage block as the storage voltage $V_{STO}$ is changed.

and DC-DC converter blocks together with the on-chip capacitor $C_{DD}$ is 1.6 $mm^2$. The majority of this area is occupied by the resistors of the various reference ladders employed in this design. $C_{DD}$ is a 470 pF capacitance which was obtained using gate-oxide capacitors. A commercially available thermoelectric device (model G1-1.0-127-1.27) [7] from Tellurex was used to perform certain measurements reported in this section. The harvester has a Seebeck coefficient of around 25 mV/K of temperature difference applied across it. The chip is directly fed from the harvester with no other external clocks or references required. For other measurements, a voltage source with a series resistance was used as the equivalent to replace the thermoelectric harvester (see Fig. 1).

Fig. 10 shows an oscilloscope waveform of the different voltages in the thermoelectric energy harvesting circuit for a 50 mV input open-circuit voltage. This corresponds to 2 K temperature difference applied across the thermal harvester. On the application of a small amount of force, the mechanical switch turns on and off kick starting the energy transfer. $V_{DD}$ initially jumps above 1 V triggering the startup block and turning ON the clock and reference generator units. The startup block then brings $V_{DD}$ up to 1.8 V and keeps it regulated there. The ripple seen on the $V_{DD}$ line is high initially because of the small value of $C_{DD}$. Once $V_{DD}$ goes above 1.8 V, the storage block is enabled as seen by the rise in $V_{STO}$. The start block keeps $V_{DD}$ close to 1.8 V

| Parameter | Lhermet [11] | Doms [5] | Carlson [6] | EnOcean [14] | This work |
|---|---|---|---|---|---|
| **Process** | 0.35μm | 0.35μm | 0.13μm | n/a | 0.35μm |
| **Min. input voltage** | 1V | 0.6V | 20mV | 20mV | 25mV (35mV to startup) |
| **External voltage?** | None | 2V battery | Minimum of 650mV | None | None |
| **Output Voltage** | 1.75V-4.3V | 2V | 1V regulated | 4V-4.5V | 1.8V regulated |
| **Peak efficiency** | 50% (just boost converter) | 70% (just boost converter) | 52% (end-to-end) | 20% (end-to-end) | 58% (end-to-end) |
| **Maximum Power Tracking?** | No | Yes | No | No | Yes |

Fig. 13. Comparison of the state-of-the-art power management circuits for thermal energy harvesting. End-to-end efficiency is defined as the ratio of the power provided to the output to the maximum power available from the thermal harvester.

while powering up the storage block. Only after $V_{STO}$ reaches 2.4 V is the DC-DC buck converter block enabled to power $V_L$. While $V_L$ is getting powered, the voltage $V_{STO}$ stays almost constant at 2.4 V. Once $V_L$ reaches 1.8 V, the capacitors $C_L$ and $C_{\rm DD}$ are shorted together. From this point on, both $V_{\rm DD}$ and $V_L$ have overlapping waveforms. The $V_{\rm DD}$ and $V_L$ waveforms are staggered a bit vertically in the oscilloscope plot to let the reader see both the waveforms. After $V_L$ reaches 1.8 V, $V_{STO}$ begins to rise further till the input power just matches the power consumed by the output load. The ripple voltage on $V_{\rm DD}$ is very high initially due to the small value of $C_{\rm DD}$. The ripple is much reduced once $V_L$ reaches 1.8 V at which point $V_{\rm DD}$ and $V_L$ are shorted. The entire startup sequence from the mechanical input to the load voltage coming up to 1.8 V takes 18 ms. It will be smaller if a higher input voltage is applied. The thermal harvesting chip was measured to startup from voltages down to 35 mV.

Fig. 11 shows the measured power obtained at the output of the DC-DC converter as the input voltage of the thermoelectric harvester is changed. This measurement was done with a 5 Ω input series resistance. The output power shown takes into account the power required to generate the clock and the reference voltages. It is the electrical power available out of the $V_L$ supply. The energy harvesting circuit can output a 1.8 V load voltage from input voltages as low as 25 mV. This means that the whole circuit once started can extract power from a thermal harvester with only 1 K temperature difference across its sides. The startup voltage required is 35 mV which corresponds to 1.5 K of temperature difference. Overall the circuit achieves a maximum end-to-end efficiency of 58%. The end-to-end efficiency is defined as the ratio of the power obtained at the load to the maximum power available from the thermal harvester. The majority of the loss is in the storage block where the high voltage transformation ratios lead to significant conduction loss in the switches. The energy harvesting circuit is able to output 10 $\mu$W of electrical power with 25 mV input voltage. The output power obtained using the thermal harvesting circuit and the overall end-to-end electrical efficiency compares favorably with published work on thermal energy harvesting interface circuits. The work presented in [5] achieves a conversion efficiency of 60–70% in the DC-DC converter with a startup voltage of 600 mV. The circuit presented works of a battery voltage of 2 V. The work presented in [11] uses a 1 V thermal input voltage and achieves a DC-DC converter efficiency of 5–50% depending on the input current. Both the efficiency numbers quoted above are of the DC-DC converter and not the end-to-end efficiency taking into account the maximum output power possible.

Fig. 12 shows the power obtained at the output of the storage capacitor with change in storage voltage. This measurement was taken with a 100 mV input with a 5 Ω series resistance. It can be seen that the power obtained at the output of the storage block is nearly independent of the storage voltage $V_{STO}$, which can be anywhere between 2.4 V–5 V. The storage block is able to output a total power of 300 $\mu$W which is 60% of the available power with a 100 mV input. The constancy of efficiency with change in storage voltage validates the operation of the closed loop zero-current switching technique, which helps in turning off the boost converter switches at the right instant irrespective of the input and output voltage.

Fig. 13 shows a comparison of the performance of the presented circuit with other state-of-the-art thermal energy harvesting circuits. The current circuit was implemented in a 0.35 $\mu$m digital CMOS process and can startup from 35 mV without the application of any external voltage. Once started, the circuit can operate down to 25 mV of input voltage. The present system provides a complete energy management solution with the storage block incorporated in the chip. A regulated 1.8 V output is provided by the chip with an overall end-to-end efficiency of 58% which is the best reported to date. High efficiency is obtained through efficient low quiescent current control circuits and by tracking the maximum power point of the harvester.

## IX. Conclusion

Thermoelectric elements can be used to harvest thermal energy present in everyday surroundings like on the human body to provide usable electrical power. The voltage output by the thermoelectric elements is proportional to the temperature difference across them. This is of concern while using thermal harvesters in body-worn applications as the voltage output by the

harvester is only 25–50 mV in most cases. Techniques have been provided in this paper that allows circuits to interface directly with and extract power out of thermoelectric generators. This enables load circuits like processors and radios to operate directly of the thermoelectric generator without the aid of a battery. A complete power management solution was provided that could extract electrical power efficiently from the harvester independent of the input voltage conditions. Also, the availability of a regulated output voltage makes it easier to interface to load circuits on the other end. With the help of closed-loop control techniques and a maximum power tracking method which just involved setting the clock frequency to a specific value, the energy processing circuit is able to maintain efficiency over a wide range of load voltage and process variations. The power management solution provided is specifically targeted for ultra-low-power applications.

## ACKNOWLEDGMENT

The authors thank Prof. J. Lang and Dr. H. Li for valuable help with this project.

## REFERENCES

[1] S. Roundy, P. Wright, and J. Rabaey, *Energy Scavenging for Wireless Sensor Networks With Special Focus on Vibrations*. Boston, MA: Kluwer Academic, 2003.

[2] M. Kishi, H. Nemoto, T. Hamao, M. Yamamoto, S. Sudou, M. Mandai, and S. Yamamoto, "Micro thermoelectric modules and their application to wristwatches as an energy source," in *Proc. Int. Conf. Thermoelectrics*, 1999, pp. 301–307.

[3] S. Lineykin and S. Ben-Yaakov, "Modeling and analysis of thermoelectric modules," *IEEE Trans. Ind. Appl.*, vol. 43, no. 2, pp. 505–512, Mar.–Apr. 2007.

[4] P. Spies, M. Pollak, and G. Rohmer, "Energy harvesting for mobile communication devices," in *Proc. 29th INTELEC*, Oct. 2007, pp. 481–488.

[5] I. Doms, P. Merken, R. Mertens, and C. Van Hoof, "Integrated capacitive power-management circuit for thermal harvesters with output power 10 to 1000 $\mu$W," in *IEEE ISSCC Dig. Tech. Papers*, Feb. 2009, pp. 300–301.

[6] E. Carlson, K. Strunz, and B. Otis, "20 mV input boost converter for thermoelectric energy harvesting," in *IEEE Symp. VLSI Circuits Dig. Tech. Papers*, Jun. 2009, pp. 162–163.

[7] Tellurex Thermoelectric Energy Harvester—G1-1.0-127-1.27, Tellurex [Online]. Available: http://www.tellurex.com

[8] J. Damaschke, "Design of a low-input-voltage converter for thermoelectric generator," *IEEE Trans. Ind. Appl.*, vol. 33, no. 5, pp. 1203–1207, Sep, 1997.

[9] B. Shen, R. Hendry, J. Cancheevaram, C. Watkins, M. Mantini, and R. Venkatasubramanian, "DC-DC converter suitable for thermoelectric generator," in *Proc. Int. Conf. Thermoelectrics*, Jun. 2005, pp. 529–531.

[10] J. Kimball, T. Flowers, and P. Chapman, "Low-input-voltage, low-power boost converter design issues," *IEEE Power Electron. Lett.*, vol. 2, no. 3, pp. 96–99, Sep. 2004.

[11] H. Lhermet, C. Condemine, M. Plissonnier, R. Salot, P. Audebert, and M. Rosset, "Efficient power management circuit: From thermal energy harvesting to above-IC microbattery energy storage," *IEEE J. Solid-State Circuits*, vol. 43, no. 1, pp. 246–255, Jan. 2008.

[12] Y. K. Ramadass and A. P. Chandrakasan, "An efficient piezoelectric energy-harvesting interface circuit using a bias-flip rectifier and shared inductor," *IEEE J. Solid-State Circuits*, vol. 45, no. 1, pp. 189–204, Jan. 2010.

[13] Y. K. Ramadass, "Energy Processing Circuits for Low-Power Applications," Ph.D. dissertation, Massachusetts Institute of Technology, Cambridge, MA, Jun. 2009.

[14] *EnOcean ECT 100 User Manual V. 2.2*.

**Yogesh K. Ramadass** received the B.Tech. degree in electronics and electrical communication engineering from the Indian Institute of Technology, Kharagpur, India, in 2004 and the M.S. and Ph.D. degrees in electrical engineering from the Massachusetts Institute of Technology, Cambridge, MA, in 2006 and 2009.

He is currently a design engineer with Texas Instruments working on energy harvesting/processing circuits and low power DC-DC converters.

Dr. Ramadass was awarded the President of India Gold Medal in 2004, was a co-recipient of the Jack Kilby Best Student Paper award at ISSCC 2009 and the Beatrice Winner award for editorial excellence at ISSCC 2007, and won the 7th International Low Power Design Contest award at ISLPED 2007. He was a recipient of the 2008–2009 Intel Foundation Ph.D. Fellowship.

**Anantha P. Chandrakasan** (F'04) received the B.S., M.S., and Ph.D. degrees in electrical engineering and computer sciences from the University of California, Berkeley, in 1989, 1990, and 1994, respectively.

Since September 1994, he has been with the Massachusetts Institute of Technology, Cambridge, where he is currently the Joseph F. and Nancy P. Keithley Professor of Electrical Engineering. He is the Director of the MIT Microsystems Technology Laboratories. His research interests include low-power digital integrated circuit design, wireless microsensors, ultra-wideband radios, and emerging technologies. He is a coauthor of *Low Power Digital CMOS Design* (Kluwer Academic Publishers, 1995), *Digital Integrated Circuits* (Pearson Prentice-Hall, 2003, 2nd edition), and *Sub-threshold Design for Ultra-Low Power Systems* (Springer, 2006). He is also a co-editor of *Low Power CMOS Design* (IEEE Press, 1998), *Design of High-Performance Microprocessor Circuits* (IEEE Press, 2000), and *Leakage in Nanometer CMOS Technologies* (Springer, 2005).

Dr. Chandrakasan was a co-recipient of several awards including the 1993 IEEE Communications Society's Best Tutorial Paper Award, the IEEE Electron Devices Society's 1997 Paul Rappaport Award for the Best Paper in an EDS publication during 1997, the 1999 DAC Design Contest Award, the 2004 DAC/ISSCC Student Design Contest Award, the 2007 ISSCC Beatrice Winner Award for Editorial Excellence and the ISSCC Jack Kilby Award for Outstanding Student Paper (2007, 2008, 2009). He received the 2009 Semiconductor Industry Association (SIA) University Researcher Award He has served as a technical program co-chair for the 1997 International Symposium on Low Power Electronics and Design (ISLPED), VLSI Design '98, and the 1998 IEEE Workshop on Signal Processing Systems. He was the Signal Processing Sub-committee Chair for ISSCC 1999-2001, the Program Vice-Chair for ISSCC 2002, the Program Chair for ISSCC 2003, the Technology Directions Sub-committee Chair for ISSCC 2004-2009, and the Conference Chair for ISSCC 2010. He is the Conference Chair for ISSCC 2011. He was an Associate Editor for the IEEE JOURNAL OF SOLID-STATE CIRCUITS from 1998 to 2001. He served on SSCS AdCom from 2000 to 2007 and he was the meetings committee chair from 2004 to 2007.